

Millennial climatic fluctuations are key to the structure of last glacial ecosystems

Article

Published Version

Creative Commons: Attribution 3.0 (CC-BY)

Huntley, B., Allen, J. R. M., Collingham, Y. C., Hickler, T., Lister, A. M., Singarayer, J., Stuart, A. J., Sykes, M. T. and Valdes, P. J. (2013) Millennial climatic fluctuations are key to the structure of last glacial ecosystems. PLoS ONE, 8 (4). e61963. ISSN 1932-6203 doi: 10.1371/journal.pone.0061963 Available at <https://centaur.reading.ac.uk/34546/>

It is advisable to refer to the publisher's version if you intend to cite from the work. See [Guidance on citing](#).

To link to this article DOI: <http://dx.doi.org/10.1371/journal.pone.0061963>

Publisher: PLOS

All outputs in CentAUR are protected by Intellectual Property Rights law, including copyright law. Copyright and IPR is retained by the creators or other copyright holders. Terms and conditions for use of this material are defined in the [End User Agreement](#).

www.reading.ac.uk/centaur

CentAUR

Central Archive at the University of Reading

Reading's research outputs online

Millennial Climatic Fluctuations Are Key to the Structure of Last Glacial Ecosystems

Brian Huntley^{1*}, Judy R. M. Allen¹, Yvonne C. Collingham¹, Thomas Hickler^{2,3}, Adrian M. Lister⁴, Joy Singarayer⁵, Anthony J. Stuart¹, Martin T. Sykes⁶, Paul J. Valdes⁵

1 School of Biological and Biomedical Sciences, Durham University, Durham, United Kingdom, **2** Biodiversity and Climate Research Centre (BiK-F), Senckenberg Gesellschaft für Naturforschung, Frankfurt am Main, Germany, **3** Department of Physical Geography, Goethe-University Frankfurt, Frankfurt am Main, Germany, **4** Palaeontology Department, Palaeontology Research Division, Natural History Museum, London, United Kingdom, **5** School of Geographical Sciences, University of Bristol, Bristol, United Kingdom, **6** Department of Physical Geography and Ecosystem Science, Geocentrum 2, Lund University, Lund, Sweden

Abstract

Whereas fossil evidence indicates extensive treeless vegetation and diverse grazing megafauna in Europe and northern Asia during the last glacial, experiments combining vegetation models and climate models have to-date simulated widespread persistence of trees. Resolving this conflict is key to understanding both last glacial ecosystems and extinction of most of the mega-herbivores. Using a dynamic vegetation model (DVM) we explored the implications of the differing climatic conditions generated by a general circulation model (GCM) in “normal” and “hosing” experiments. Whilst the former approximate interstadial conditions, the latter, designed to mimic Heinrich Events, approximate stadial conditions. The “hosing” experiments gave simulated European vegetation much closer in composition to that inferred from fossil evidence than did the “normal” experiments. Given the short duration of interstadials, and the rate at which forest cover expanded during the late-glacial and early Holocene, our results demonstrate the importance of millennial variability in determining the character of last glacial ecosystems.

Citation: Huntley B, Allen JRM, Collingham YC, Hickler T, Lister AM, et al. (2013) Millennial Climatic Fluctuations Are Key to the Structure of Last Glacial Ecosystems. PLoS ONE 8(4): e61963. doi:10.1371/journal.pone.0061963

Editor: Jacqueline Mohan, Odum School of Ecology, University of Georgia, United States of America

Received: October 8, 2012; **Accepted:** March 15, 2013; **Published:** April 16, 2013

Copyright: © 2013 Huntley et al. This is an open-access article distributed under the terms of the Creative Commons Attribution License, which permits unrestricted use, distribution, and reproduction in any medium, provided the original author and source are credited.

Funding: The research reported was supported by grant NE/G00188X/1 awarded by the UK Natural Environment Research Council (<http://www.nerc.ac.uk/>). The funder had no role in study design, data collection and analysis, decision to publish, or preparation of the manuscript.

Competing Interests: The authors have declared that no competing interests exist.

* E-mail: brian.huntley@durham.ac.uk

Introduction

Fossil remains of mega-herbivores, including the iconic Woolly Mammoth (*Mammuthus primigenius*) and Woolly Rhinoceros (*Coelodonta antiquitatis*), show they were widespread and abundant in ice-free areas of the northern continents during the last glacial [1,2]. Such large-bodied grazers require productive ecosystems dominated by herbaceous plants. Although macrofossils indicate trees were locally present [3], pollen data indicate the glacial vegetation throughout most of Europe [4], northern Asia [5], Beringia [6] and western North America [7] was dominated by non-woody plants, and thus potentially able to support mega-herbivores. Fossil evidence, however, provides limited, if any, quantitative evidence of vegetation productivity, and hence of its capacity to sustain a grazer community.

Vegetation models provide a means to estimate structure, composition and productivity of glacial vegetation. To apply such models, however, glacial climatic conditions are required as input, in turn requiring output from GCM palaeoclimate experiments. GCM experiments made with prescribed sea surface temperatures and sea-ice extent [8] gave results that disagreed with pollen and other palaeoclimatic evidence, especially in western Europe [4,9]. When these palaeoclimate experiments were used to drive an equilibrium vegetation model, the glacial vegetation of Europe was simulated to be largely forest, a result that conflicts strongly with pollen evidence [4]. More recent experiments with fully-coupled

atmosphere–ocean GCMs [10,11] give results that conflict much less with geological evidence of last glacial climates. In parallel, dynamic vegetation models have been developed [12,13] that simulate the processes of vegetation development and its responses not only to climatic changes but also to changes in atmospheric CO₂ concentration and in seasonal solar radiation intensity. One such model, LPJ-GUESS [14], has been used to simulate last glacial vegetation of northern Eurasia [15], simulations being driven by outputs from palaeoclimate experiments made using the HadCM3 GCM [10]. Although these simulations showed generally limited forest extent before and during the LGM, productivity of woody plants in western Eurasia at the LGM was higher than expected and inconsistent with very sparse representation of trees in the pollen record. Rapid extension of simulated forest cover across Eurasia after the LGM broadly coincided with rapid geographical range reductions of previously widespread mega-herbivores, and was likely to have been a major contributor to the extinction of many [2], but relatively low simulated productivity of herbaceous plants at the LGM, especially in the west, conflicted with evidence of widespread presence and abundance of mega-herbivores.

Ice-core records show glacial climates were characterised by millennial-scale alternations between warmer interstadials and colder stadials [16]. The most extreme alternations were associated with Heinrich Events in the North Atlantic [17], during which Atlantic meridional overturning circulation appar-

ently collapsed [18]. Comparing results of the HadCM3 experiments with temperatures reconstructed for central Greenland shows that experiments using a combination of ‘slow’ forcings (orbital configuration; atmospheric composition; ice sheet extent and topography; sea-level; and land-sea mask), referred to hereafter as ‘normal’ experiments, generally match and track temperatures reconstructed for the warmest parts of interstadials [10]. In contrast, a series of ‘hosing’ experiments [10] designed to mimic Heinrich Events H1 to H5 give temperatures close to and tracking those reconstructed for stadials. LPJ-GUESS simulations driven by the normal experiments thus indicate potential vegetation of the warmest parts of interstadials. They hence give a biased view of last glacial vegetation, because peak interstadial conditions account for a minority of the time.

To investigate potential stadial vegetation, and how this differs from that of peak interstadials, we performed two series of LPJ-GUESS simulations, the first driven by the five hosing experiments and the second driven by the normal experiments for the time slices corresponding to the Heinrich Events (H1–17 ka BP; H2–24 ka BP; H3–32 ka BP; H4–38 ka BP; H5–46 ka BP). A further pair of simulations, for 6 ka BP and 120 ka BP, was performed to explore how vegetation patterns during the last interglacial may have differed from those during the Holocene; in particular, whether they were more favourable for survival of mega-herbivores, at least in East Siberia [19], during the last interglacial.

Materials and Methods

Methods for the LPJ-GUESS simulations were as in Reference [15], with the following two exceptions. Firstly, simulations were made for the entire northern hemisphere land area north of 35°N. Secondly, simulations were extended to include continental shelf areas exposed by glacial sea-level depression. To achieve the latter, 1961–90 climatic conditions were estimated for shelf areas by interpolation and/or extrapolation of the CRU CL 1.0 data [20], as described in Reference [21], and palaeoclimatic conditions inferred using the same anomaly-based approach used in the earlier work [15], thus minimising impacts of GCM biases. Results were summarised by summing simulated annual net primary productivity (ANPP) values for each grid cell and experiment for three groups of plant functional types (PFTs): trees–woody PFTs of tree stature, taken to be ≥ 3 m; shrubs–woody PFTs forming only shrubs (≤ 3 m tall) or dwarf shrubs; and herbs–non-woody PFTs.

Results

Figures 1–5 present the results for H1/17 ka BP, H2/24 ka BP, H3/32 ka BP, H4/38 ka BP and H5/46 ka BP respectively. In each case, across large areas of northern Eurasia, but especially Europe, hosing experiment climates give generally lower ANPP for trees and shrubs and higher ANPP for herbs than equivalent normal experiments. This is in much better accord with pollen evidence than is vegetation simulated for normal experiments. In contrast, hosing experiments give higher simulated tree ANPP in western North America south of the Laurentide Ice Sheet than do normal experiments. This too accords better with fossil evidence, areas of highest simulated ANPP matching areas of highest reconstructed tree density [7]. Figure 6 shows the results for 6 and 120 ka BP and indicates that East Siberia had higher ANPP of herbaceous PFTs and lower ANPP of woody PFTs during the last interglacial than during the Holocene.

Discussion

Given greater prevalence of stadial conditions, and relatively limited duration of the warmest parts of most interstadials, the contrast in simulated vegetation between hosing and normal experiments provides the key to reconciling modelled vegetation with the fossil record, and also to understanding the nature of glacial ecosystems that supported mega-herbivore communities. Under stadial conditions, ANPP of herbaceous plants was increased, whereas that of trees was much reduced, especially in Europe, and was less than that of herbs. It is likely that trees were only sparsely present in most areas, either as scattered individuals or localised stands, in a landscape dominated by productive herbaceous communities. Furthermore, tree ANPP was non-zero north of the Alps principally in central Europe, corresponding to the location of macrofossil occurrences of trees, and only Boreal tree PFTs contributed, again matching macrofossil data [3,22]. On each occasion when interstadial conditions developed, temperate trees, limited to southern Europe during the last glacial [23], would begin to expand their ranges into newly suitable areas from which they were excluded during stadials. Populations of Boreal trees able to persist north of the Alps under stadial conditions would expand across the landscape from the favourable sites in which they had survived. Late-glacial and Holocene pollen data provide a basis for estimating rates at which such expanding tree populations in turn lead to the expansion of forest or woodland cover [24,25]. Although forests or woodlands formed by a minority of taxa were able to expand at rates of between 1 and 2 km yr⁻¹, long-term average expansion rates of forests formed by most tree taxa were between 200 and 500 m yr⁻¹. Most trees hence require two to five millennia to advance the margin of the area where they form extensive forest cover by 1000 km; even the most rapid require 500 yr to achieve this distance.

Most last-glacial interstadials, however, were of short duration, especially during marine oxygen isotope Stage 2. Fifteen interstadials with discrete onset and termination have durations between 100 and 2600 yr (mode 300 yr; mean 1000 yr) [16]. At NGRIP, last glacial (14.7–76.5 b2k) $\delta^{18}\text{O}$ values are in the upper 25% of the range for that interval only 9% of the time, whereas they are in the lower half of the range 61% of the time (data file “2010-11-19 GICC05modelext for NGRIP.xls” downloaded 11/1/12 from <http://www.iceandclimate.nbi.ku.dk/data/>). Many areas simulated as more or less treeless under stadial conditions extend >1000 km from areas with higher ANPP of trees under stadial conditions. Most trees are thus unlikely to have expanded their ranges and populations sufficiently to develop the extents of forest or woodland cover potentially possible under interstadial climatic conditions, except perhaps during the longest interstadials (GI 12: 46.8–44.2 ka BP; GI 19: 72.3–70.3 ka BP; and GI 20: 76.4–74.0 ka BP). Glacial vegetation was thus, as hypothesised by Lister and Sher [26], maintained in a generally treeless but productive state across most of the northern continents as a result of what they referred to as “the constant stirring” of millennial climatic fluctuations.

These modelling results and the inferences we make from them are fully consistent with the palaeovegetation evidence from Europe for the last glacial stage. Allen and Huntley [27] reviewed the then available evidence and showed that at sites in southern Europe, south of the main mountain chains, tree pollen abundance increased to levels indicative of open woodland or wooded steppe during last glacial interstadials, whereas grasses and steppic herbs predominated during stadial intervals. During the longer and warmer interstadials between *ca.* 60,000 cal yr BP and *ca.* 30,000 cal yr BP, temperate forest trees were important

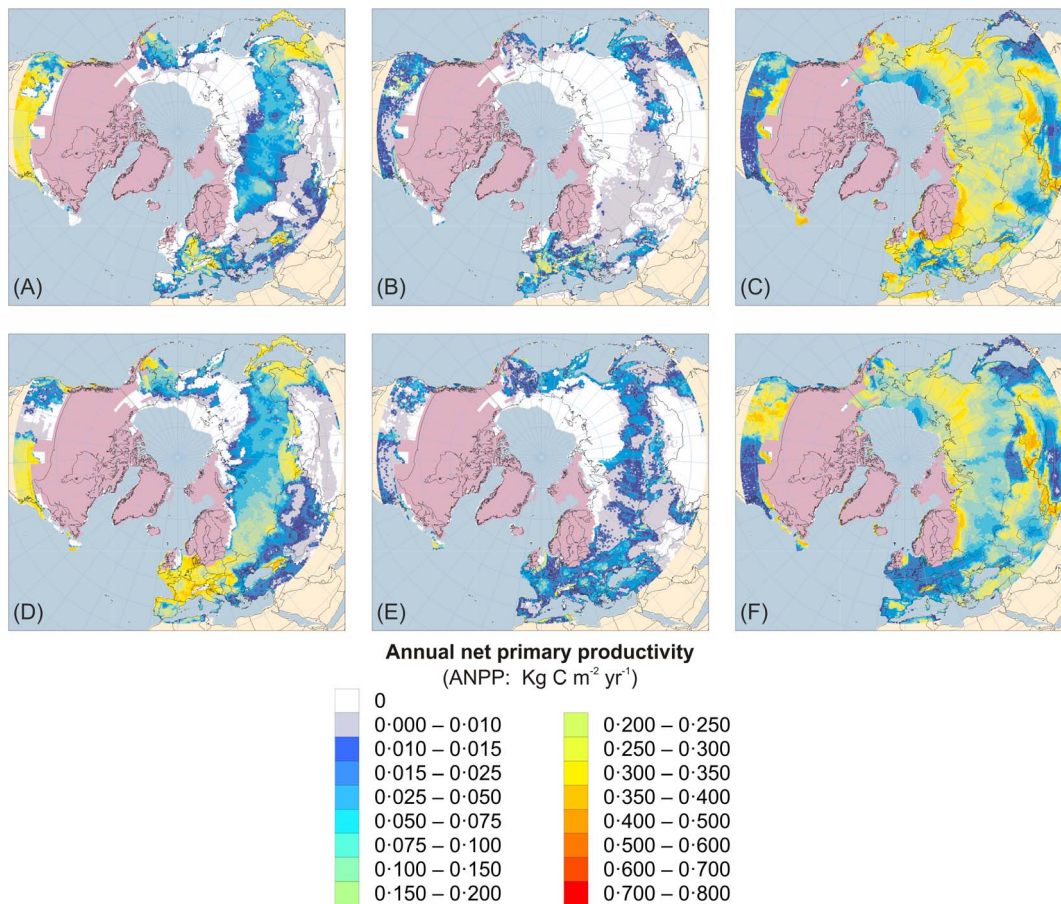


Figure 1. Tree, shrub and herb plant functional type ANPP:Heinrich Event 1 hosing experiment compared to 17 ka BP normal experiment. Annual net primary productivity (ANPP) for the aggregated tree (A and D), shrub (B and E) and herb (C and F) plant functional types (PFTs) simulated for the palaeoclimates generated by the Heinrich Event 1 hosing experiment (A–C) and the equivalent 17 ka BP normal experiment (D–F). Lilac shaded areas indicate the extent of the modelled last glacial ice sheets for 17 ka BP [38]; land area is shown for sea-level lowered by 107 m [39]. ANPP is indicated by shading of land areas: white areas have zero ANPP for that PFT; pale grey areas have non-zero but very low ANPP; shades from deep blue through cyan and pale cyan to yellow and orange indicate progressively higher ANPP as shown by the quantitative legend.
doi:10.1371/journal.pone.0061963.g001

components of the woody vegetation, whereas the shorter and colder interstadials that predominated between *ca.* 75,000 cal yr BP and *ca.* 60,000 cal yr BP, as well as between *ca.* 30,000 cal yr BP and *ca.* 14,000 cal yr BP, generally were characterised by the predominance of *Pinus* and *Juniperus* amongst the woody taxa. North of the main mountain chains, most interstadials are expressed more weakly in the palaeovegetation record. Increased amounts of tree pollen at sites in central Europe indicate development of open woodland during some of the longer and warmer intervals, although the tree taxa concerned are restricted to Boreal taxa, notably *Betula*, *Picea*, *Pinus* and *Juniperus*. In northern Europe the palaeovegetation record documents only a few of the interstadial events; they are characterised there by a predominance of herbaceous and dwarf-shrub taxa, with pollen of woody taxa infrequent, principally being very low abundances of Boreal taxa, notably *Betula*, *Pinus* and *Juniperus*, the first and last of which are likely to represent principally the shrubby taxa *B. nana* and *J. communis*. Although a few additional records, for example Reference [28], have been published since the review by Allen and Huntley [27] was undertaken, these records have not altered in any substantive way the overall picture. Forest did not extend across Europe north of the main mountain chains at any time during Marine Oxygen Isotope (MOI) stages 2–4 [29], although

during interstadials woodland or wooded steppe with temperate tree taxa extended across areas of southern Europe, especially during MOI stage 3. Even during the latter warmer and/or longer interstadials, however, only Boreal tree populations expanded in central Europe, forming open or patchy woodlands rather than extensive forest cover, whilst in northern Europe herbaceous and dwarf-shrub vegetation prevailed during these intervals.

In contrast to the last glacial, Holocene climatic fluctuations have been generally of much smaller magnitude than those during the glacial. Conditions favourable for forest development across most of northern Eurasia have prevailed throughout the Holocene. The climatic fluctuations that have occurred generally have resulted in only relatively small shifts (≤ 100 km) in the latitudinal treeline, altering the overall extent of forest cover by *ca.* 5% at most. Thus, not only have conditions favoured extensive forest development in areas where herbaceous taxa dominated glacial ecosystems [15], but forests have persisted more than ten millennia in many areas. The relative rapidity with which forests extended, compared to the rate of marginal retreat of the Laurentide and Fennoscandian Ice Sheets, resulted in a critical late-glacial to early Holocene reduction in extent of cold, productive herbaceous ecosystems upon which the mega-herbivores depended. For some, e.g. Woolly Rhinoceros–*Coelodonta antiquitatis*, extinction followed

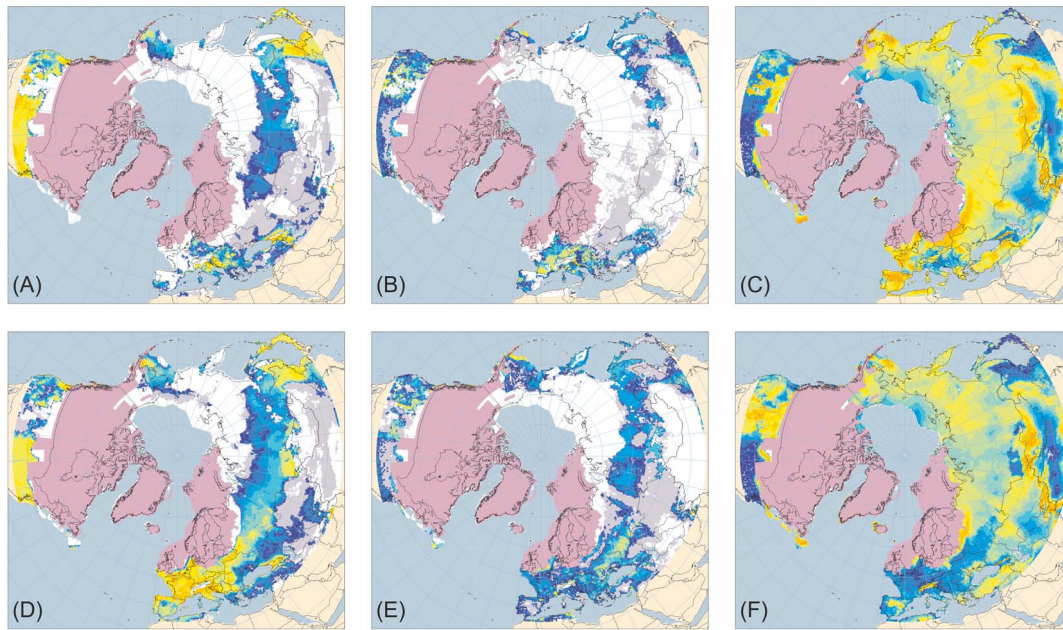


Figure 2. Tree, shrub and herb plant functional type ANPP: Heinrich Event 2 hosing experiment compared to 24 ka BP normal experiment. ANPP for the aggregated tree (A and D), shrub (B and E) and herb (C and F) plant functional types (PFTs) simulated for the palaeoclimates generated by the Heinrich Event 2 hosing experiment (A–C) and the equivalent 24 ka BP normal experiment (D–F). Lilac shaded areas indicate the extent of the modelled last glacial maximum ice sheet [38]; land area is shown for sea-level lowered by 112 m [40]. ANPP is indicated by shading of land areas: white areas have zero ANPP for that PFT; pale grey areas have non-zero but very low ANPP; shades from deep blue through cyan and pale cyan to yellow and orange indicate progressively higher ANPP (for quantitative legend see Fig. 1). doi:10.1371/journal.pone.0061963.g002

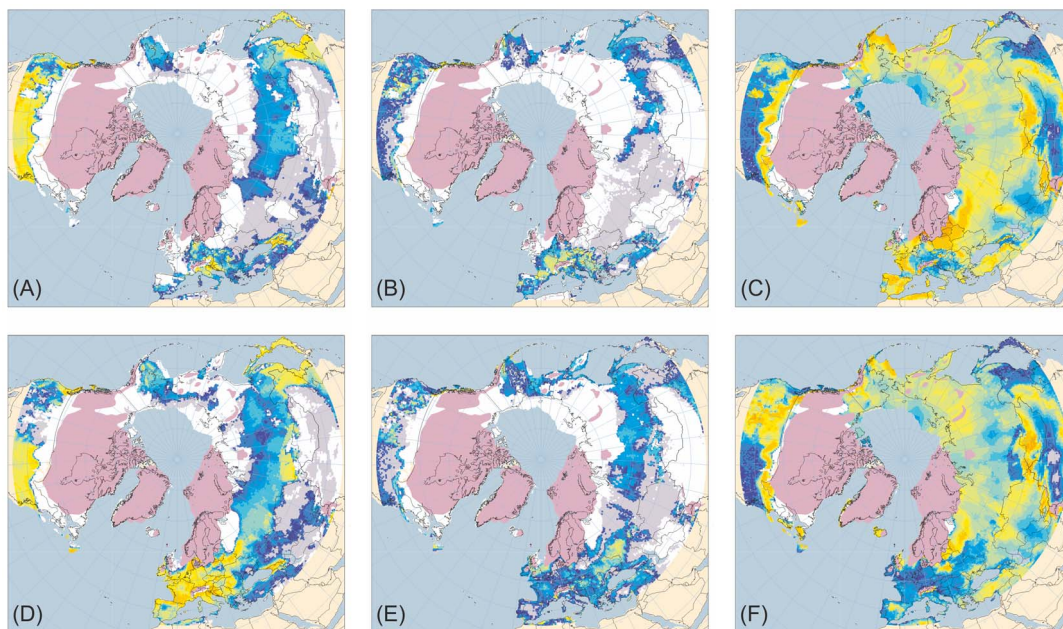


Figure 3. Tree, shrub and herb plant functional type ANPP: Heinrich Event 3 hosing experiment compared to 32 ka BP normal experiment. ANPP for the aggregated tree (A and D), shrub (B and E) and herb (C and F) plant functional types (PFTs) simulated for the palaeoclimates generated by the Heinrich Event 3 hosing experiment (A–C) and the equivalent 32 ka BP normal experiment (D–F). Lilac shaded areas indicate the extent of the ice sheets mapped for the mid-Weichselian [41]; land area is shown for sea-level lowered by 80 m [40]. ANPP is indicated by shading of land areas: white areas have zero ANPP for that PFT; pale grey areas have non-zero but very low ANPP; shades from deep blue through cyan and pale cyan to yellow and orange indicate progressively higher ANPP (for quantitative legend see Fig. 1). doi:10.1371/journal.pone.0061963.g003

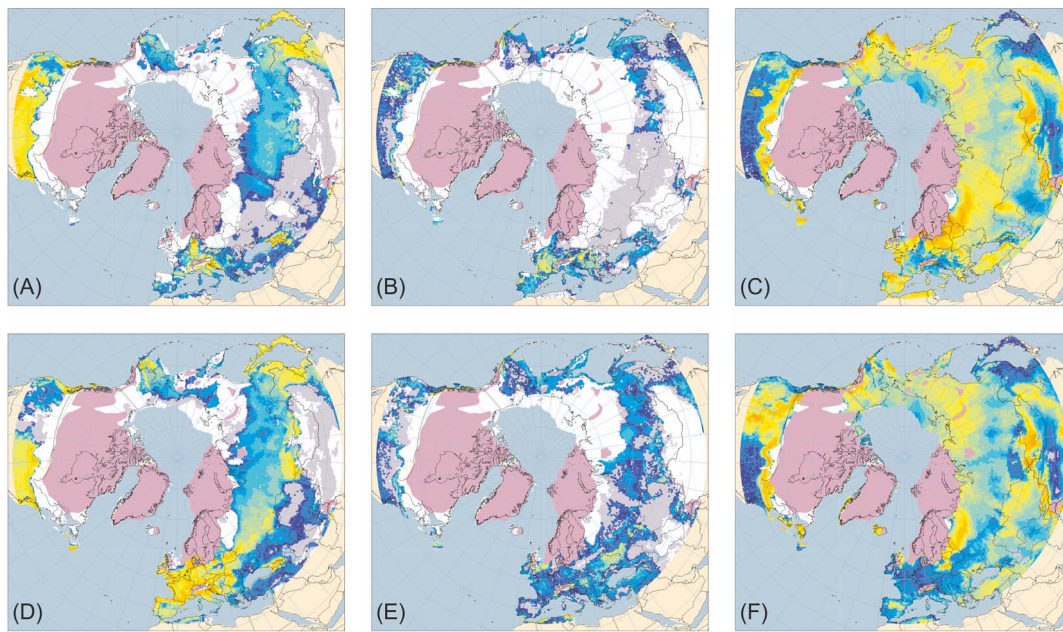


Figure 4. Tree, shrub and herb plant functional type ANPP: Heinrich Event 4 hosing experiment compared to 38 ka BP normal experiment. ANPP for the aggregated tree (A and D), shrub (B and E) and herb (C and F) plant functional types (PFTs) simulated for the palaeoclimates generated by the Heinrich Event 4 hosing experiment (A–C) and the equivalent 38 ka BP normal experiment (D–F). Lilac shaded areas indicate the extent of the ice sheets mapped for the mid-Weichselian [41]; land area is shown for sea-level lowered by 80 m [40]. ANPP is indicated by shading of land areas: white areas have zero ANPP for that PFT; pale grey areas have non-zero but very low ANPP; shades from deep blue through cyan and pale cyan to yellow and orange indicate progressively higher ANPP (for quantitative legend see Fig. 1). doi:10.1371/journal.pone.0061963.g004

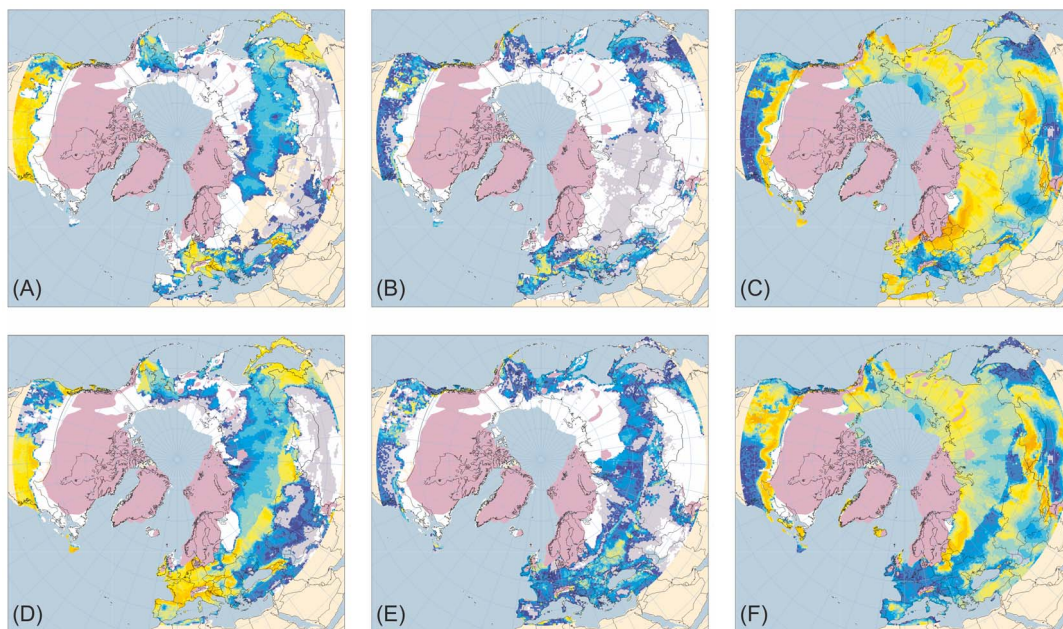


Figure 5. Tree, shrub and herb plant functional type ANPP: Heinrich Event 5 hosing experiment compared to 46 ka BP normal experiment. ANPP for the aggregated tree (A and D), shrub (B and E) and herb (C and F) plant functional types (PFTs) simulated for the palaeoclimates generated by the Heinrich Event 5 hosing experiment (A–C) and the equivalent 46 ka BP normal experiment (D–F). Lilac shaded areas indicate the extent of the ice sheets mapped for the mid-Weichselian [41]; land area is shown for sea-level lowered by 80 m [40]. ANPP is indicated by shading of land areas: white areas have zero ANPP for that PFT; pale grey areas have non-zero but very low ANPP; shades from deep blue through cyan and pale cyan to yellow and orange indicate progressively higher ANPP (for quantitative legend see Fig. 1). doi:10.1371/journal.pone.0061963.g005

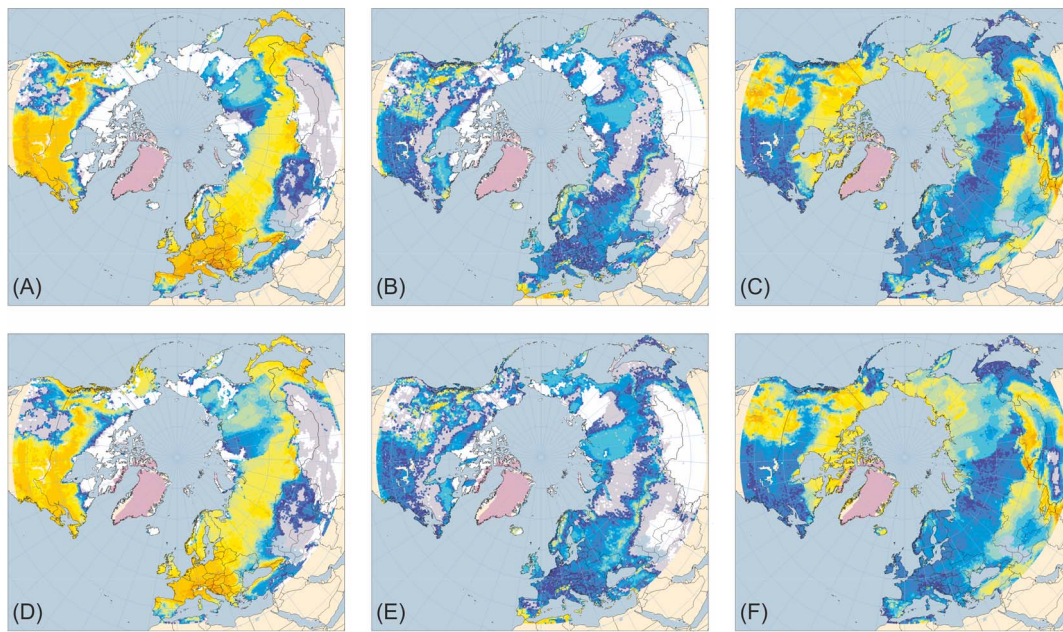


Figure 6. Tree, shrub and herb plant functional type ANPP: 120 ka BP (Last interglacial) compared to 6 ka BP (Holocene 'optimum'). ANPP for the aggregated tree (A and D), shrub (B and E) and herb (C and F) plant functional types (PFTs) simulated for the palaeoclimates generated by the 120 ka BP (last interglacial) experiment (A–C) and the 6 ka BP (Holocene 'optimum') experiment (D–F). Lilac shaded areas on the maps for 6 ka BP indicate the extent of the modelled ice sheets for that time [38] whilst those on the maps for 120 ka BP show the extent of ice sheets mapped for the Holocene by Ehlers and Gibbard [41]; land area is shown for sea-levels of -8 m [39] and $+2$ m [40] for 6 ka BP and 120 ka BP, respectively. ANPP is indicated by shading of land areas: white areas have zero ANPP for that PFT; pale grey areas have non-zero but very low ANPP; shades from deep blue through cyan and pale cyan to yellow and orange indicate progressively higher ANPP (for quantitative legend see Fig. 1).
doi:10.1371/journal.pone.0061963.g006

initial forest expansion after the LGM [2]. Others, e.g. Woolly Mammoth–*Mammuthus primigenius*, also contracted their range greatly around this time but persisted to the mid-Holocene, in this case in restricted areas of suitable habitat on islands north of Siberia [30] and in the Bering Sea [31], but eventually went extinct. Yet others of the glacial mega-herbivore assemblage are extant, e.g. Musk Oxen–*Ovibos moschatus*, but show genetic evidence of a severe bottleneck between the LGM and late Holocene [32], only occupying their principal modern range in Greenland after the mid-Holocene [33].

In contrast to the Holocene, last interglacial palaeovegetation evidence from East Siberia indicates continuous forest cover was less extensive in that region [5,34] during that interval. Consistent with this, simulated vegetation in East Siberia for 120 ka BP shows generally higher ANPP of herbs and lower ANPP of woody PFTs, especially trees, than at 6 ka BP (Fig. 6). Notwithstanding higher simulated tree ANPP in many Boreal and temperate forest areas at 120 ka BP than at 6 ka BP, the Arctic treeline generally is simulated at a lower latitude at 120 ka BP than at 6 ka BP. Local exceptions include an area of higher tree ANPP at 120 ka BP close to the East Siberian north coast, corresponding to evidence of occurrence of trees in that area [34]. In contrast to the Holocene, last interglacial ecosystems in East Siberia were thus probably able to support mega-herbivore communities. Such contrasts between interglacials are to be expected, given the differences in orbital forcing and hence in climatic conditions. Furthermore, the contrast in vegetation characteristics of East Siberia between the last interglacial and the Holocene provides support for the argument that the particular nature of the environmental changes after the last glacial maximum and during the early Holocene was

the primary factor in causing the extinctions of many larger vertebrates of Eurasia during that period, rather than the coincidental increase in the geographical range, abundance and/or technological status of anatomically modern humans [35].

Climate is once again changing rapidly [36], with implications for biodiversity that are of global concern. Our results provide the basis for either optimism or pessimism, depending upon predictions of how climate is likely to evolve over coming centuries. If the recent and continuing perturbation of atmospheric composition, and associated global mean temperature increase, is an excursion, with a return to pre-industrial levels of greenhouse gases in the atmosphere within the next century or so, then, as during the last glacial, we can expect the limited response rates of many ecosystems, and forest systems especially, to provide a buffer against more extreme impacts upon biodiversity. If, on the other hand, as seems very likely, atmospheric composition remains in a perturbed state, and global mean temperature as a result increases to a value more than *ca.* 2°C warmer than its pre-industrial value, we can expect major ecosystem disruption and associated extinctions [37], as occurred with the shift to persistently warmer conditions at the onset of the Holocene.

Author Contributions

Provided expertise on megafauna: AJS AML. Contributed to revision and editing of the final manuscript: BH JRMA YCC TH AML JS AJS MTS PJV. Conceived and designed the experiments: BH AML PJV JRMA. Performed the experiments: JS PJV JRMA YCC. Analyzed the data: BH. Contributed reagents/materials/analysis tools: MTS TH JS PJV. Wrote the paper: BH.

References

1. FAUNMAP Working Group (1996) Spatial response of mammals to late Quaternary environmental fluctuations. *Science* 272: 1601–1606.
2. Stuart AJ, Lister AM (2012) Extinction chronology of the woolly rhinoceros *Coelodonta antiquitatis* in the context of late Quaternary megafaunal extinctions in northern Eurasia. *Quaternary Science Reviews* 51: 1–17.
3. Binney HA, Willis KJ, Edwards ME, Bhagwat SA, Anderson PM, et al. (2009) The distribution of late-Quaternary woody taxa in northern Eurasia: evidence from a new macrofossil database. *Quaternary Science Reviews* 28: 2445–2464.
4. Huntley B, Alfano MJ, Allen JRM, Pollard D, Tzedakis PC, et al. (2003) European vegetation during marine oxygen isotope Stage 3. *Quaternary Research* 59: 195–212.
5. Sher AV, Kuzmina SA, Kuznetsova TV, Sulerzhitsky LD (2005) New insights into the Weichselian environment and climate of the East Siberian Arctic, derived from fossil insects, plants, and mammals. *Quaternary Science Reviews* 24: 533–569.
6. Zazula GD, Schweger CE, Beaudoin AB, McCourt GH (2006) Macrofossil and pollen evidence for full-glacial steppe within an ecological mosaic along the Bluefish River, eastern Beringia. *Quaternary International* 142: 2–19.
7. Williams JW (2003) Variations in tree cover in North America since the last glacial maximum. *Global and Planetary Change* 35: 1–23.
8. Barron E, Pollard D (2002) High-resolution climate simulations of oxygen isotope stage 3 in Europe. *Quaternary Research* 58: 296–309.
9. Alfano MJ, Barron EJ, Pollard D, Huntley B, Allen JRM (2003) Comparison of climate model results with European vegetation and permafrost during oxygen isotope stage three. *Quaternary Research* 59: 97–107.
10. Singarayer JS, Valdes PJ (2010) High-latitude climate sensitivity to ice-sheet forcing over the last 120 kyr. *Quaternary Science Reviews* 29: 43–55.
11. Kjellström E, Brandefelt J, Naslund JO, Smith B, Strandberg G, et al. (2010) Simulated climate conditions in Europe during the Marine Isotope Stage 3 stadial. *Boreas* 39: 436–456.
12. Stith S, Smith B, Prentice IC, Arneth A, Bondeau A, et al. (2003) Evaluation of ecosystem dynamics, plant geography and terrestrial carbon cycling in the LPJ dynamic global vegetation model. *Global Change Biology* 9: 161–185.
13. Cramer W, Bondeau A, Woodward FI, Prentice IC, Betts RA, et al. (2001) Global response of terrestrial ecosystem structure and function to CO₂ and climate change: results from six dynamic global vegetation models. *Global Change Biology* 7: 357–373.
14. Smith B, Prentice IC, Sykes MT (2001) Representation of vegetation dynamics in the modelling of terrestrial ecosystems: comparing two contrasting approaches within European climate space. *Global Ecology and Biogeography* 10: 621–637.
15. Allen JRM, Hickler T, Singarayer JS, Sykes MT, Valdes PJ, et al. (2010) Last glacial vegetation of northern Eurasia. *Quaternary Science Reviews* 29: 2604–2618.
16. Wolff EW, Chappellaz J, Blunier T, Rasmussen SO, Svensson A (2010) Millennial-scale variability during the last glacial: The ice core record. *Quaternary Science Reviews* 29: 2828–2838.
17. Bond G, Broecker W, Johnsen S, McManus J, Labeyrie L, et al. (1993) Correlations between climate records from North Atlantic sediments and Greenland ice. *Nature* 365: 143–147.
18. Seidov D, Maslin M (1999) North Atlantic deep water circulation collapse during Heinrich events. *Geology* 27: 23–26.
19. Sher A (1997) Late-Quaternary extinction of large mammals in northern Eurasia: A new look at the Siberian contribution. In: Huntley B, Cramer W, Morgan AV, Prentice HC, Allen JRM, editors. Past and future rapid environmental changes: The spatial and evolutionary responses of terrestrial biota. Berlin: Springer-Verlag. pp. 319–339.
20. New M, Hulme M, Jones P (1999) Representing twentieth-century space–time climate variability. Part I: Development of a 1961–90 mean monthly terrestrial climatology. *Journal of Climate* 12: 829–856.
21. Huntley B, Allen JRM, Barnard P, Collingham YC, Holliday PR (2013) Species' distribution models indicate contrasting late-Quaternary histories for southern and northern hemisphere bird species. *Global Ecology and Biogeography* 22: 277–288.
22. Willis KJ, van Andel TH (2004) Trees or no trees? The environments of central and eastern Europe during the Last Glaciation. *Quaternary Science Reviews* 23: 2369–2387.
23. Bhagwat SA, Willis KJ (2008) Species persistence in northerly glacial refugia of Europe: a matter of chance or biogeographical traits? *Journal of Biogeography* 35: 464–482.
24. Huntley B, Birks HJB (1983) An atlas of past and present pollen maps for Europe: 0–13000 B.P. Cambridge: Cambridge University Press. 667 p.
25. Davis MB (1983) Holocene vegetational history of the eastern United States. In: Wright HE, Jr, editor. Late Quaternary Environments of the United States. Minneapolis: University of Minnesota Press. pp. 166–181.
26. Lister AM, Sher AV (1995) Ice cores and mammoth extinction. *Nature* 378: 23–24.
27. Allen JRM, Huntley B (2000) Weichselian palynological records from southern Europe: correlation and chronology. *Quaternary International* 73/74: 111–125.
28. Müller UC, Pross J, Bibus E (2003) Vegetation response to rapid climate change in Central Europe during the past 140,000 yr based on evidence from the Fürstmoos pollen record. *Quaternary Research* 59: 235–245.
29. Martinson DG, Pias NG, Hays JD, Imbrie J, Moore TC, Jr, et al. (1987) Age dating and the orbital theory of the ice ages: development of a high-resolution 0 to 300,000-year chronostratigraphy. *Quaternary Research* 27: 1–29.
30. Vartanyan SL, Garutt VE, Sher AV (1993) Holocene Dwarf Mammoths from Wrangel-Island in the Siberian Arctic. *Nature* 362: 337–340.
31. Guthrie RD (2004) Radiocarbon evidence of mid-Holocene mammoths stranded on an Alaskan Bering Sea island. *Nature* 429: 746–749.
32. MacPhee RDE, Tikhonov AN, Mol D, Greenwood AD (2005) Late Quaternary loss of genetic diversity in muskox (*Ovibos*). *BMC Evolutionary Biology* 5: 1–13.
33. Bennike O, Andreassen C (2005) Radiocarbon dating of musk-ox (*Ovibos moschatus*) remains from northeast Greenland. *Polar Record* 41: 305–310.
34. Kienast F, Wetterich S, Kuzmina S, Schirmer L, Andreev AA, et al. (2011) Paleontological records indicate the occurrence of open woodlands in a dry inland climate at the present-day Arctic coast in western Beringia during the Last Interglacial. *Quaternary Science Reviews* 30: 2134–2159.
35. Barnosky AD, Koch PL, Feranec RS, Wing SL, Shabel AB (2004) Assessing the causes of Late Pleistocene extinctions on the continents. *Science* 306: 70–75.
36. Trenberth KE, Jones PD, Ambenje P, Bojariu R, Easterling D, et al. (2007) Observations: Surface and Atmospheric Climate Change. In: Solomon S, Qin D, Manning M, Chen Z, Marquis M et al., editors. Climate Change 2007: The Physical Science Basis Contribution of Working Group I to the Fourth Assessment Report of the Intergovernmental Panel on Climate Change. Cambridge, United Kingdom and New York, NY, USA: Cambridge University Press. pp. 235–336.
37. Parry ML, Canziani OF, Palutikof JP, Co-authors (2007) Technical Summary. Climate Change 2007: Impacts, Adaptation and Vulnerability. In: Parry ML, Canziani OF, Palutikof JP, Linden PJ, Hanson CE, editors. Contribution of Working Group II to the Fourth Assessment Report of the Intergovernmental Panel on Climate Change. Cambridge, UK: Cambridge University Press. pp. 23–78.
38. Peltier WR (2004) Global glacial isostasy and the surface of the ice-age earth: The ICE-5G (VM2) model and GRACE. *Annual Review of Earth and Planetary Sciences* 32: 111–149.
39. Fairbanks RG (1989) A 17,000-year glacio-eustatic sea level record: Influence of glacial melting rates on the Younger Dryas event and deep-ocean circulation. *Nature* 342: 637–642.
40. Bard E, Hamelin B, Fairbanks RG (1990) U-Th ages obtained by mass-spectrometry in corals from Barbados–Sea-level during the past 130,000 years. *Nature* 346: 456–458.
41. Ehlers J, Gibbard PL, editors (2004) Quaternary glaciations: Extent and chronology (3 Vols.). Amsterdam: Elsevier Science. 488, 450 & 433 p.